The chemokine receptors CXCR1 and CXCR2 couple to distinct G protein-coupled receptor kinases to mediate and regulate leukocyte functions

Sandeep K. Raghuwanshi[§], **Yingjun Su**[†,*], **Vandana Singh**[§], **Katherine Hayes**[§], **Ann Richmond**[†,*], and **Ricardo M. Richardson**[§]

[§]Julius L. Chambers Biomedical/Biotechnology Research Institute and Department of Biology, North Carolina Central University, Durham, NC 27707

[†]Department of Veterans Affairs, Nashville, Tennessee, 37212

[*]Department of Cancer Biology, Vanderbilt University School of Medicine, Nashville, TN 37232

Abstract

The chemokine receptors, CXCR1 and CXCR2, couple to $G\alpha i$ to induce leukocyte recruitment and activation at sites of inflammation. Upon activation by CXCL8, these receptors become phosphorylated, desensitized and internalized. In this study we investigated the role of different G protein-coupled receptor kinases (GRKs) in CXCR1- and CXCR2-mediated cellular functions. To that end, shRNA was used to inhibit GRK 2, 3, 5 and 6 in RBL-2H3 cells stably expressing CXCR1 or CXCR2, and CXCL8-mediated receptor activation and regulation were assessed. Inhibition of GRK2 and GRK6, respectively, increased CXCR1 and CXCR2 resistance to phosphorylation, desensitization and internalization, and enhanced CXCL8-induced phosphoinositide hydrolysis and exocytosis *in vitro*. GRK2 depletion diminished CXCR1-induced ERK1/2 phosphorylation but had no effect in CXCR2-induced ERK1/2 phosphorylation. GRK6 depletion had no significant effect on CXCR1 function. However, peritoneal neutrophils from mice deficient in GRK6 (GRK6$^{-/-}$) displayed an increase in CXCR2-mediated G-protein activation, but *in vitro* exhibited a decrease in chemotaxis, receptor desensitization and internalization relative to wild type (GRK6$^{+/+}$) cells. In contrast, neutrophil recruitment *in vivo* in GRK6$^{-/-}$ mice was increased in response to delivery of CXCL1 through the air-pouch model. In a wound closure assay, GRK6$^{-/-}$ mice showed enhanced myeloperoxidase activity, suggesting enhanced neutrophil recruitment, and faster wound closure as compared to GRK6$^{+/+}$ animals. Taken together, the results indicate that CXCR1 and CXCR2 couple to distinct GRK isoforms to mediate and regulate inflammatory responses. CXCR1 predominantly couples to GRK2, whereas CXCR2 interacts with GRK6 to negatively regulate receptor sensitization and trafficking, thus affecting cell signaling and angiogenesis.

Keywords

Address correspondence and reprint requests to Dr. Ricardo M. Richardson, Julius L. Chambers Biomedical/Biotechnology Research Institute, North Carolina Central University, 1801 Fayetteville Street, Durham, NC 27707. mrrichardson@nccu.edu.

Introduction

Interleukin-8 (IL-8/CXCL8) is a member of the CXC subfamily of chemokines that binds two seven transmembrane G-protein-coupled receptors (GPCRs), CXCR1 and CXCR2 to mediate and regulate leukocyte accumulation and activation at sites of inflammation (1, 2). CXCR1 interacts predominantly with CXCL8, whereas CXCR2 also binds CXCL1, 2, 3, 5 & 7 (3). Upon activation, both receptors couple to pertussis toxin (Ptx) sensitive $G\alpha i$ proteins to activate phospholipase C (PLC), resulting in the generation of the intracellular messenger diacylglycerol (DAG) and inositol 1,4,5-triphosphate (IP_3). Following CXCL8 activation, CXCR1 and CXCR2 become desensitized and internalized (4, 5). In contrast, $G\beta\gamma$ subunits activate phosphotidyl inositol -3-kinase (PI3K), leading to phosphorylation of PI (4,5) diphosphate to form PI (3,4,5) tris-phosphate which activates many signal transduction pathways required for motility, growth, and gene expression.

Phosphorylation of GPCRs by G protein-coupled receptor kinases (GRKs) and recruitment of clathrin binding adaptor proteins to the cell membrane are prerequisite for receptor desensitization (6, 7). Thus far, seven GRKs (GRK 1 to 7) have been identified and characterized (8). GRK1 and GRK7 are exclusively expressed in the visual system, retinal rods and cones, respectively (9). GRK2, GRK3, GRK5 and GRK6 are expressed in most mammalian cell types, whereas GRK4 expression has been detected only in the testis, kidney and cerebellum (9, 10). Genetic deletion in mouse and suppression of expression of specific GRKs in transfected cell lines by small interfering RNA (siRNA) targeting have indicated that GPCRs may couple to specific GRKs to modulate distinct, as well similar, cellular responses (11–14).

To date, the role of GRK isoforms in chemokine receptor functions remains ill-defined. Decreased expression of GRK2 correlates with increased cellular responses to the CC receptors CCR2 and CCR5 (15–17). CCR7 was shown to couple to both GRK3 and GRK6 to undergo receptor phosphorylation and desensitization, but only GRK6 phosphorylation led to MAP kinase activation (18). Neutrophils deficient in GRK6 displayed increased CXCR4 activation and resistance to desensitization (19). Busilo et al (20) have also shown that GRK2 and GRK3 are critical for CXCR4 desensitization and post-endocytic signaling. Altogether these data suggest that the chemokine receptors couple to specific GRKs to mediate and regulate cellular functions.

Previous studies from our laboratory (4, 5) and others (21–23) have shown that GRK-mediated phosphorylation of specific amino acid residues in the cytoplasmic tails of CXCR1 and CXCR2 is critical for β-arrestin association, receptor internalization, and receptor-induced post-endocytic signals in some cell types. In this study we sought to determine the role of different GRKs in CXCR1 and CXCR2-mediated cellular functions. To that end, rat basophilic leukemia (RBL-2H3) cell lines in which expression of GRK 2, 3, 5 or 6 were suppressed by shRNA, and mouse models of inflammation deficient in GRK6 were generated to assess receptor activation and regulation. Taken together, the results indicate that, upon activation by CXCL8, CXCR1 and CXCR2 interact with distinct GRK isoforms to modulate leukocyte functions.

Materials and Methods

Materials

$[^{32}P]$Orthophosphate (8500–9120 Ci/mmol), myo-$[2-^3H]$inositol (24.4 Ci/mmol) and $[^{125}I]$-CXCL8 were purchased from Perkin Elmer. IL-8 (CXCL8) and CXCL1 were obtained from Peprotech (Rocky Hill, NJ). Indo-1 AM, Geneticin (G418) and all tissue culture reagents were purchased from Invitrogen (Gaithersburg, MD). Monoclonal 12CA5 antibody, protein

G-agarose and protease inhibitors were purchased from Roche (Indianapolis, IN). Anti-Human IL-8RA (CXCR1) and IL-8RB (CXCR2) antibodies were purchased from BD Pharmigen (San Jose, CA). Anti-GRK 2/3 and anti-GRK5/6 were obtained from Millipore (Billerica, MA). Rabbit anti-ERK1/2 and anti-phospho-ERK1/2 antibodies were purchased from Cell Signaling (Beverly, MA). Mission shRNA Plasmid DNA (pLKO.1-puro) for GRK subtypes were purchased from Sigma Life Sciences (St. Louis, MO) or obtained from Dr Hydar Ali laboratory (University of Pennsylvania, Philadelphia, PA). All other reagents were from commercial sources.

Cell culture and transfection

RBL-2H3 cells were maintained as monolayer cultures in Dulbecco's modified Eagle's medium (DMEM) supplemented with 15% heat inactivated fetal bovine serum, 2 mM glutamine, penicillin (100 units/ml), and streptomycin (100 mg/ml) (24). RBL-2H3 cells (1×10^7) were transfected by electroporation with 20 μg of pcDNA3 containing the receptor cDNAs, and Geneticin-resistant cells were cloned into single cells and confirmed by fluorescence-activated cell sorter (FACS) analysis. The levels of protein expression were monitored by FACS analysis (25). For shRNA mediated gene silencing, RBL-2H3 cells (1×10^7 cells) were transfected by electroporation with 20 μg of mission pLKO.1-puro containing shRNA for GRK2, GRK3, GRK5, GRK6, or control plasmid. Puromycin-resistant cells were cloned into single cell by limiting dilution method. Levels of mRNA transcript and protein expression were monitored by Real-Time PCR and western blotting.

FACS analysis

For flow cytometric analysis, RBL cells were detached by Versene treatment, washed with HEPES buffered Hanks' balanced salt solution (HHBSS) and resuspended in the same medium. Cells ($1-5 \times 10^6$ cells) were incubated with anti-CXCR1 or anti-CXCR2 antibodies (1 μg/ml) in a total volume of 400 μl of HHBSS for 60 min at 4°C. The cells were then washed and incubated with fluorescein (FITC)-antimouse IgG for 60 min at 4°C. Cells were then washed and analyzed for cell surface expression of the receptor on a Beckton Dickenson FACScan cytometer (5).

Radioligand binding assays and receptor internalization

For receptor internalization, RBL-2H3 cells were sub-cultured overnight in 24-well plates (0.5×10^6 cells/well) in growth medium. Cells were then rinsed with Dulbecco's modified Eagles medium supplemented with 20 mM HEPES, pH 7.4, and 10 mg/ml BSA, then incubated with ligand for 0–60 min at 37°C. Then cells were washed with ice-cold PBS and ^{125}I-CXCL8 binding (0.1 nM) was carried out as described previously (5). Nonspecific radioactivity bound was determined in the presence of 500 nM un-labelled CXCL8 (26).

Phosphoinositide hydrolysis, β-hexosaminidase release and calcium measurement

RBL-2H3 cells were subcultured overnight in 96-well culture plates (50,000 cells/well) in inositol-free medium supplemented with 10% dialyzed fetal bovine serum and 1 μCi/ml [^{3}H]inositol. The generation of inositol phosphates was determined as reported (24, 27). For calcium mobilization, cells (5×10^6) were washed with HEPES buffered saline and loaded with 1 μM Indo-acetoxymethyl ester in the presence of 1 μM pluronic acid for 30 minutes at room temperature. The cells were then washed with HEPES and resuspended in 1.5 ml of Siriganian buffer. Intracellular calcium increase in the presence or absence of ligands was measured as described previously (28).

Receptor Phosphorylation

Receptor phosphorylation was performed as described previously (5, 25). RBL-2H3 cells (5×10^6) expressing the receptors were incubated with [^{32}P]orthophosphate (150 μCi/dish) for 90 min. Then labeled cells were stimulated with the indicated ligands for 5 minutes at 37°C. Cells were then washed with ice-cold PBS and solubilized in 1 ml of radioimmunoassays buffer (RIPA) containing 50 mM Tris-HCl (pH 7.5), 150 mM NaCl, 1% Nonidet P-40, 0.5% sodium deoxycholate, and 0.1% SDS. Cell lysates were immunoprecipitated with specific antibodies against the N-terminus of CXCR1 or CXCR2 and analyzed by SDS electrophoresis and visualized by autoradiography.

Measurement of ERK Activity

For ERK activity, RBL-2H3 cells (3×10^6) expressing the CXCR1 or CXCR2, or peritoneal neutrophils from GRK6$^{-/-}$ mice and control littermates (GRK6$^{+/+}$) were washed three times with PBS and then resuspended in PBS containing CXCL8 (100 nM) for different periods of time at 37 °C. The reactions were stopped with ice-cold PBS; cells were collected by centrifugation, lysed with RIPA, and assayed for protein concentration as described previously (29). Equal amounts of protein (20 μg) from each sample were resolved by 10% SDS-PAGE, transferred to a nitrocellulose membrane, and probed with antibody against either ERK1/2 or phospho-ERK1/2. Detection was carried out with horseradish peroxidase-conjugated sheep anti-mouse antibody and by ECL.

Animals

All experiments were approved by and confirmed to the guidelines of the Animal Care Committee of North Carolina Central University, Durham, NC, Vanderbilt University School of Medicine, and/or Meharry Medical College. Animals were housed five per cage in a room at 22 ± 5°C with an alternate 12 h light-dark cycle. GRK6 deficient mice (C57/BL6 background) were kindly provided by Dr. Robert J. Lefkowitz (Howard Hughes Medical Institute, Duke University Medical Center, Durham NC 27710). Male and female mice were evaluated and controls were age and sex matched littermates. All the mice were genotyped at the age of three weeks; DNA samples were prepared from the tail tips with DNeasy tissue kit from Qiagen Inc. USA and subjected to triplex PCR as described (30, 31).

Peritoneal recruitment of neutrophils

Zymosan was prepared in PBS to a final concentration of 1 mg/ml and 1.0 ml was injected into the peritoneum of control and GRK6 deficient mice. Mice were euthanized by CO_2 asphyxiation and the peritoneal cavity was lavaged at 4 h post-injection with 8 ml of ice-cold RPMI containing 2% fetal bovine serum and 2 mM EDTA. Cells were collected by centrifugation, counted, stained with Diff-Quick to assess the percentage of neutrophils (32).

Membrane preparations

Zymosan-elicited peritoneal neutrophils were resuspended in homogenizing buffer containing 25 mM Tris Buffer (pH 7.6), 5 mM MgCl2 and proteases inhibitors (1μl/ml); and homogenized for 30 s with a Polytron. The homogenate was centrifuged at $150 \times g$ for 5 min and the supernatant was collected. The procedure was repeated twice and the pooled supernatant was centrifuged at $10,000 \times g$ for 10 min. The pellet was resuspended in the same buffer (1 mg of protein/ml) and stored at −80°C until use.

Intracellular Ca^{2+} mobilization, receptor internalization, GTPase activity and chemotaxis

Zymosan-elicited peritoneal neutrophils (3×10^6 cells) were washed with HEPES-buffered saline and loaded with 1 μM Indo-1-AM for 30 min at room temperature. The cells were washed and resuspended in 1.5 ml of HEPES-buffered saline and intracellular Ca^{2+}

mobilization was measured as described (32). For receptor internalization, 5×10^5 neutrophils were resuspended in 250 μl of HBSS containing 25 mM HEPES and 0.1% BSA. Cells were treated with recombinant murine CXCL1 (100 nM) at 37°C for different time periods. Reactions were stopped by adding 1 ml of ice-cold HBSS followed by centrifugation at 1,000 rpm for 2 min. Then cells were washed three times and assayed for [^{125}I]CXCL1 binding as previously described (32). For GTPase activity, membranes (10 μg of membrane preparations/assay) were assayed as described (32, 33) in the presence and absence of 1 μM recombinant murine CXCL1. For chemotaxis neutrophils (~50,000) were incubated at 37°C with different concentrations of ligands. Chemotaxis was assessed in 48-well microchemotaxis chambers using polyvinylpyrrolidone-free 8-μm pore size membranes as described previously (29). The results are representative of three separate experiments

Murine skin air pouch model of inflammation

GRK6$^{-/-}$ and littermate control mice (6–8 wk) were anesthetized with isofluorane, and dorsal air pouches were raised by injecting 3 ml of sterile air s.c. on days 0 and 3 as described previously (34–36). On day 6, the mice were anesthetized with isofluorane and inflammation in the air pouch was induced by local injection of recombinant murine CXCL1 (100 pmol) dissolved in 0.5 ml of sterile PBS. Mice were sacrificed 4 h after CXCL1 injection by CO2 asphyxiation, and air pouches were lavaged three times with 3 ml of PBS. Cells were collected by centrifugation at 2000 rpm for 5 min at room temperature. The supernatants were removed, and the cells were resuspended in 10 ml of PBS and counted. Aliquots of the cell suspension were stained with Wright-Giemsa and enumerated by light microscopy (~90% of the exudates are neutrophils).

Mouse Skin Excisional Wounding Procedures

Excisional punch wounds were made as described previously with slight modifications (32, 37). GRK6$^{-/-}$ and Wild type mice (6–8 wk) were anesthetized with an intraperitoneal injection of ketamine (100 mg per kg body weight) and xylazine (10 mg per kg body weight) (Fort Dodge Animal Health, Fort Dodge, IA). The dorsal surface of the mouse was cleaned, shaved, and sterilized with betadine solution (Purdue Frederick, Norwalk, CT) and 70% ethanol. Two full-thickness excisional wounds were made in the dorsal paravertebral region with 4 mm diameter punch (Acu-Punch, Fort Lauderdale, FL). Wounds were covered and kept under occlusion by Spray Bandage (Curad, Beiersdorf Inc., Wilton, CT). Analgesics (Buprenex, Reckitt & Colman Pharmaceuticals Inc., Richmond, VA) were administered i.p. with dosage of 4.5 μg per kg body weight. All wounds were visually monitored daily for signs of infection.

Myeloperoxidase assay

Myeloperoxidase (MPO) activity was assayed as described previously (37, 38). Briefly, wound tissues from post-wounding days 1, 2 and 3 were harvested, snap frozen in liquid nitrogen, and homogenized in 1 ml phosphate buffer containing 0.5% hexadecyl trimethyl ammonium bromide (HTAB) in 50 mM phosphate buffer, pH 6.0. HTAB is a detergent that releases MOP from primary granules of neutrophils. After sonication on ice for 15 sec (Sonic Model 300, Fisher Scientific), tissue homogenates were centrifuged at $20,000 \times g$ for 20 min at 4°C. The supernatants were collected and their protein concentrations were measured using the Bio-Rad protein determination assay. Aliquots of the supernatant containing equivalent amounts of 50 μg protein were mixed with 500 μl of potassium phosphate buffer (50 mM, pH 6.0) containing 0.2% of O- Dianisidine hydrochloride (Sigma Chemical Co., St. Louis, MO) and 0.0005% H_2O_2. The reaction was initiated by the addition of hydrogen peroxide. The change in absorbance at 490 nm during a 2-min reaction period was measured spectrophotometrically, using the Beckman-DU 7000 (Beckman Coulter Inc., Fullerton, CA). The absorbance values were compared for each aliquot of wound tissue

lysate from wild type and GRK6$^{-/-}$ mice. The MPO values of non-wounded skin tissues from each genotype served as controls.

Wound closure analysis

Wounds were collected on post-wounding days 3, 5, 7, and 10. Each wound was centrally bisected, embedded in paraffin, sectioned at six microns followed by staining with Gomori's Trichrome. For wild type or GRK6$^{-/-}$ mouse, 8 wound tissues from 4 mice were excised and analyzed for each time point. The percentage of wound resurfacing was assessed by morphometric analysis (39, 40) on tissue slide images using Image Pro Plus software.

Statistical analyses

Results are expressed as mean ± SEM. Statistical differences between groups were determined by Student's two-tailed paired t-test and the statistical difference was claimed for $p < 0.05$.

Results

Role of GRKs in CXCR1 and CXCR2 desensitization

To determine the role of GRKs in CXCR2 regulation RBL-2H3 cells stably expressing CXCR2 were transiently transfected with Mission pLKO.1-puro containing shRNA for GRK2, GRK3, GRK5, GRK6, or control plasmid. Forty eight hour post-transfection, cells were analyzed by RT-PCR (data not shown) and immunoblotting. As shown in figure 1-A expression of GRK2, GRK3, GRK5 and GRK6 were inhibited by 90–95% relative to control cells. For receptor desensitization, the peak of CXCL8-induced intracellular Ca^{2+} mobilization was measured in cells pretreated with 10 nM CXCL8 and compared to that of untreated cells. Pretreatment of RBL-CXCR1 (Fig. 1-B, left column, mock) or RBL-CXCR2 (Fig. 1-B, middle column, mock) cells desensitized response to a second dose by ~63% (Fig. 1-C, mock) and ~75% (Fig. 1-D, mock), respectively. Loss of GRK2 expression (GRK2$^{-/-}$), but not loss of GRK3 (GRK3$^{-/-}$), GRK5 (GRK5$^{-/-}$) or GRK6 (GRK6$^{-/-}$), significantly increased CXCR1 resistance to desensitization (~10% versus ~63% desensitization for GRK2$^{-/-}$ and mock cells, respectively), relative to control cells (Fig. 1-B and 1-C). On the other hand, GRK6$^{-/-}$ cells (but not GRK2$^{-/-}$, GRK3$^{-/-}$ or GRK5$^{-/-}$ cells) exhibited a significant increase in CXCR2 resistance to desensitization (~25% versus ~75% desensitization for GRK6$^{-/-}$ and mock cells, respectively; Figs. 1-B and 1-D).

In addition to CXCL8, CXCR2 interacts with CXCL1, 2, 3, 5, 6 & 7 to mediate cellular responses (41). To further assess the specificity of the CXCR2/GRK6 interaction we also measured CXCL1-induced receptor desensitization in RBL-CXCR2 cells deficient in GRKs (Fig. 1-B, right column). As shown in figure 1-E, only GRK6$^{-/-}$ cells displayed a significant increase in receptor resistance to desensitization (~15% versus ~91% desensitization for GRK6$^{-/-}$ and control mock cells, respectively). These results mirrored the ones obtained with CXCL8 and indicated that the effect of GRK6 deficiency is likely receptor specific.

Effect of GRK2 and GRK6 inhibition on CXCL8-induced receptor activation and regulation

To further assess the specificity of GRKs in receptor activation and regulation, puromycin resistant RBL-CXCR1 (Fig. 2-A) and RBL-CXCR2 (Fig. 2-B) in which GRK2 (CXCR1-GRK2$^{-/-}$ and CXCR2-GRK2$^{-/-}$) and GRK6 (CXCR1-GRK6$^{-/-}$ and CXCR2-GRK6$^{-/-}$) expression were stably suppressed, were generated by single cell cloning and confirmed by real time PCR (data not shown) and immunoblotting (Fig. 2-C). The dose-response of CXCL8-induced β-hexosaminidase release was measured to assess receptor activation. Maximum responses were ~35% and ~23% of total for CXCR1-GRK6$^{+/+}$ (Fig 3-A) and CXCR2-GRK6$^{+/+}$ (Fig 3-B), respectively. GRK6 inhibition had no effect on CXCR1-

mediated exocytosis (Fig 3-A) but caused a ~40% increase in response to CXCR2 (Fig. 3-B). Absence of GRK6 decreased CXCR2 phosphorylation (Fig. 3-D, right panel, lane 8 versus lane 6) and internalization (Fig. 3-C), with no effect on CXCR1 (Figs. 3-C; and 3-D, left panel)

The dose-response of CXCL8-induced phosphoinositide (PI) hydrolysis and β-hexosaminidase release was also measured in GRK2 deficient cells. As shown in Figure 4, CXCR1-GRK2$^{-/-}$ cells exhibited marked increase in PI hydrolysis (~35%) (Fig. 4-A), and β-hexosaminidase release (~40%) (Fig. 4-C) relative to control CXCR1-GRK2$^{+/+}$ cells. GRK2 inhibition had no effect on CXCR2-mediated responses (Fig. 4, B and D).

Attenuation of GRK2 also increased CXCR1 resistance to phosphorylation (Fig. 4-F, left panel, lane 4 versus lane 2) and internalization (Fig. 4-E), but had no effect in CXCR2 (Fig. 4E and 4-F, right panel, lanes 8 versus lane 6) relative to control GRK2$^{+/+}$ cells.

Effect of GRK2 and GRK6 in CXCL8-induced ERK1/2 activation

To determine the effect of GRK2 and GRK6 in MAP kinase activation RBL-CXCR1 and RBL-CXCR2 were stimulated with CXCL8 (100 nM) for different periods of time and cells lysates were assayed for ERK1/2 phosphorylation. As previously shown (25, 33), CXCR1 and CXCR2 induced time-dependent ERK1/2 phosphorylation (Fig. 5). GRK2 depletion (GRK2$^{-/-}$) significantly inhibited CXCR1-mediated ERK1/2 phosphorylation (Fig. 5-A and 5-C) with no significant effect on CXCR2 (Fig. 5-B and 5-D). GRK6 knockdown had no significant effect on CXCR1 or CXCR2-mediated ERK1/2 phosphorylation (Fig. 5 A-D).

Effect of GRK6 deletion in leukocyte functions

To further determine the effect of GRK6 inhibition on CXCR2 functions, zymosan-induced peritonitis was used to recruit neutrophils into the peritoneal cavity of GRK6 deficient mice (GRK6$^{-/-}$) and littermates (GRK6$^{+/+}$). Membranes were prepared and assayed for murine CXCL1-induced G protein activation. Membrane preparations from GRK6$^{-/-}$ peritoneal neutrophils displayed a robust increase (~40%) in CXCL1-mediated response (~1.3 pmol Pi released/mg protein) relative to GRK6$^{+/+}$ (~0.7 pmol Pi released/mg protein) (Fig. 6-A).

CXCL1-induced intracellular Ca^{2+} mobilization in peritoneal neutrophils was also measured to assess receptor desensitization. As shown in Fig. 6-B, pretreated neutrophils from GRK6$^{+/+}$ animals showed a ~70% decrease in CXCL1-mediated Ca^{2+} mobilization relative to untreated cells (225±25 and 69±27 nM for control and pretreated cells, respectively). Cells from GRK6$^{-/-}$ animals only displayed a ~20% desensitization (244±41 and 197±59 nM for control and pretreated cells, respectively, which did not reach statistical significance). These results mirrored the one obtained with CXCR2-GRK6$^{-/-}$ RBL cells and indicated that deletion of GRK6 increased CXCR2 resistance to desensitization.

Receptor internalization was also assessed in cells pretreated with CXCL1 (100 nM) for different periods of time (Fig. 6-C). GRK6$^{+/+}$ cells showed a rapid decrease in receptor binding (~95% after 30 min of pretreatment). CXCR2 from GRK6$^{-/-}$ cells, however, was more resistant to internalization (~75% after 30 min of pretreatment). CXCL1-mediated chemotaxis *in vitro* was significantly inhibited in peritoneal neutrophils from GRK6$^{-/-}$ animals relative to control GRK6$^{+/+}$ cells (Fig. 6-D).

We next determined the effect of GRK6 inhibition in CXCR2-mediated MAP kinase activation by measuring CXCL1 induced ERK1/2 phosphorylation (Fig. 7-A). GRK6$^{+/+}$ neutrophils showed a rapid (~23% at 1 min), but transient increase in CXCL1-induced ERK1/2 phosphorylation (Fig. 7-B, open circles). The response in GRK6$^{-/-}$ cells, however, was delayed (~10 % at 1 min) but sustained (Fig. 7-B, closed circles). The transient effect

observed at ~1 min in GRK6$^{-/-}$ cells, however, was not statistically significant (p>.05) relative to control (GRK6$^{+/+}$ cells).

Role of GRK6 in CXCR2-mediated neutrophil migration <u>in vivo</u>

Deletion of βarr2 inhibited CXCL1-mediated chemotaxis *in vitro* but enhanced neutrophil infiltration *in vivo* into the air pouch model of skin inflammation (32). To determine whether GRK6 deletion affected neutrophil migration *in vivo*, air pouches were created in GRK6$^{-/-}$ deficient mice and their littermates (GRK6$^{+/+}$). PBS induced neutrophil recruitment in GRK6$^{+/+}$ mice (~1.6×10^6 cells) was similar to that of GRK6$^{-/-}$ animals (~1.8×10^6 cells) (Fig. 8-A, open bars). By contrast, injection of CXCL1 (100 pmol) into the air pouch 6 days after it was raised induced greater neutrophil accumulation (~5.7×10^6 cells) in GRK6$^{-/-}$ mice relative to control GRK6$^{+/+}$ animals (~3.1×10^6 cells) (Fig. 8-A, closed bars) (p<0.05).

Neutrophil infiltration was further determined by MPO assays performed on excisional wound tissue extracts. MPO activity of wild type and GRK6$^{-/-}$ mouse wounds increased sharply at 24 h post-wounding, and was sustained over post-wound day 3 (Fig. 8-B). The MPO activity in wounds from GRK6$^{-/-}$ mice, however, was significantly higher (~1 and ~2 fold increase post-wounding day 1 and 2, respectively) than that of wounds from wild type mice (Fig. 8-B). This was followed by a marked decrease in MPO activity to the level exhibited in wounds from wild type mice at post-wounding day 3.

Wound re-epithelialization was also increased in GRK6$^{-/-}$ mice relative to wild type animals. The percentages of epidermal re-surfacing for GRK6$^{+/+}$ mouse wounds at days 3, 5, and 7 were 37%, 68%, and 97%, respectively. Wound resurfacing percentages from GRK6$^{-/-}$ mice was significantly increased to 58% at day 3 (p < 0.05). Wounds from both genotypes were similar at days 5 and 7 and were each completely re-epithelialized by post-wounding day 10 (Fig. 8-C).

Discussion

CXCR1 and CXCR2 bind the proangiogenic ELR-positive (ELR$^+$) chemokines to mediate cellular responses including chemotaxis and angiogenesis. These responses are regulated by phosphorylation of the receptors at specific serine and threonine residues of the carboxyl terminus leading to uncoupling of the receptor from G protein thereby promoting receptor desensitization and down-regulation (11). CXCR1 and CXCR2 are phosphorylated via two mechanisms: a protein kinase C (PKC)-dependent and a GRK-dependent (4, 28, 42). The GRKs are known to phosphorylate the agonist-occupied receptor to promote arrestin recruitment and receptor internalization (10). Upon CXCL8 activation, CXCR1 internalizes slowly (~45% after 60 min) but recovers rapidly (~100% after 90 min), whereas CXCR2 internalizes rapidly (~95% after 5–10 min) but recovers slowly (~35 % after 90 min) at the cell surface (4, 5, 42–45). This distinction appears to play a critical role in the ability of the receptors to activate certain leukocytes responses including respiratory burst, cross-regulatory and post-endocytic signals (4, 5). Thus, defining the role of specific GRK isoforms in CXCR1 and CXCR2 activation and regulation is essential to the understanding of the distinct roles played by these receptors in inflammation. The results herein have identified two GRKs, GRK2 and GRK6, as critical kinases in the regulation of CXCL8-mediated cellular functions. First, respective suppression of GRK2 and GRK6 expression significantly increased CXCR1 and CXCR2 resistance to CXCL8-mediated receptor phosphorylation, desensitization (p<0.01) and internalization (p<0.05) (Figs. 1, 3 & 4). Second, as a consequence of GRK2 or GRK6 inhibition, both receptors displayed increased CXCL8-induced cellular responses, including PI hydrolysis and β-hexosaminidase release, but decreased ERK1/2 activation (Figs. 3, 4 & 5). Third, consistent with the results obtained

in RBL cells, peritoneal neutrophils from mice deficient in GRK6 expression exhibited significant increase in murine CXCR2-mediated G protein activation, receptor resistance to desensitization and internalization, but decrease in chemotaxis relative to cells from wild type GRK6$^{+/+}$ mice (Fig. 6).

In contrast to the decrease in chemotaxis observed *in vitro*, CXCL1-induced neutrophil accumulation into dorsal air pouch generated in GRK6$^{-/-}$ mice showed a two fold increase relative to control GRK6$^{+/+}$ animals (Fig. 8, A). Peritoneal neutrophils from mice deficient in βarrestin-2 expression (βarr2$^{-/-}$) also displayed decreased chemotaxis *in vitro* but increased recruitment into the air pouch model of inflammation (32). In both cases, the knockout cells showed increase CXCR2-mediated G protein-activation in membranes and receptor resistance to desensitization and internalization. Previous studies with transfected cell lines expressing phosphorylation deficient mutants of CXCR1 and CXCR2 showed that decreased receptor internalization correlated with decreased CXCL8-mediated chemotaxis but increased receptor-mediated G protein activation, second messenger production and exocytosis (5). Thus, the increase in CXCL1-induced neutrophil accumulation into the air pouch relative to wild type animals could be a consequence of the increased receptor activity that resulted in greater secretion of proteases and tissue permeability, thereby facilitating cell migration. A second explanation could be the difference among the air-pouch and the transwell assays used to measure chemotaxis. A third explanation could be that β-arrestin play a negative regulatory role, such that loss of this negative regulator results in enhanced chemotaxis that is more apparent *in vivo* than *in vitro*, possibly involving the microenvironment of the cells. Interestingly, as was the case with βarr2$^{-/-}$ mice (32), cutaneous excisional wounds in GRK6$^{-/-}$ animals displayed significant increase in MPO activity in the wound bed as well as rapid wounds re-epithelialization relative to GRK6$^{+/+}$ (Fig. 8, B and C) which likely indicate greater CXCR2-induced angiogenesis.

It was recently shown that inhibition of GRK6 in mast cells promoted ERK1/2 phosphorylation but attenuated C3aR-mediated degranulation (46). Inhibition of GRK6 in the RBL-2H3 mast cell line, however, had no significant effect in CXCR2-mediated ERK1/2 phosphorylation but enhanced β-hexosaminidase release in response to CXCL8 (Figs. 3 and 5). This difference likely indicates that the two receptors couple to distinct pathways to activate MAP kinase and mediate granule release in mast cells. Suppression of β-arrestin1 (βarr-1) expression in mast cells inhibited C3aR-mediated ERK1/2 activation (47). In contrast, inhibition of βarr-2, not βarr-1, was shown to decrease CXCR2-induced ERK1/2 activation (48). In addition, attenuation of GRK6 had no effect in C3aR desensitization but increased CXCR2 resistance to receptor phosphorylation, desensitization and internalization [(46) and Fig. 3C, D and Fig. 6 B and C].

Although GRK2 and GRK6 appeared to be the important GRKs in CXCR1 and CXCR2 regulation, respectively, the possibility exists that other isoform(s) may participate in receptor mediated post-endocytic signals. Indeed, GRK2 depletion significantly attenuated CXCR1-mediated ERK1/2 activation, whereas response to CXCR2 was affected by neither GRK2 nor GRK6 inhibition (Fig 5). The V2 vasopressin receptor was shown to couple to GRK2 and GRK3 to undergo receptor phosphorylation and desensitization, but to GRK5 and GRK6 to mediate post-endocytic signals including ERK1/2 activation (49). C3aR desensitization and internalization are also mediated through GRK2 and GRK3 dependent pathways whereas exocytosis and MAP kinase activation are modulated through GRK5 and GRK6 (46). CCR7 was also shown to couple to both GRK3 and GRK6 to undergo phosphorylation and desensitization but only GRK6 phosphorylation led to MAP kinase activation (18). CXCR4 was shown to couple to GRK2, GRK3 and GRK6 to modulate ERK1/2 activation (20).

Inhibition of GRK2 in RBL-2H3 cells totally prevented CXCR1 endocytosis (~40% versus ~100% for GRK2$^{+/+}$ and GRK2$^{-/-}$ cells, respectively, after 60 min; Fig. 4E) whereas the effect of GRK6 depletion on CXCR2 was partial (~5% versus ~65% for GRK6$^{+/+}$ and GRK6$^{-/-}$ cells, respectively, after 60 min; Fig. 3C). Previous studies using transfected cells lines expressing wild type and mutant receptors have shown that in addition to GRK-mediated receptor phosphorylation and arrestin-dependent internalization, CXCR2 also internalizes through a receptor phosphorylation/arrestin-independent process (5, 32). Thus, this partial inhibition of receptor internalization may be due to the receptor ability to scaffold to other adaptor protein such as adaptor protein-2 (AP2) and the heat shock cognate/heat shock protein 70-interacting protein (HIP) to internalize (50, 51). Supporting that contention is that in mouse embryonic fibroblast (MEF) deficient in both βarr1 and βarr2 (βarr1/2$^{-/-}$), CXCR2 internalization was simply delayed relative to control MEF βarr1/2$^{+/+}$) (48).

In summary, the data herein indicate that GRK2 and GRK6 negatively regulate CXCR1- and CXCR2-mediated neutrophil functions. Two questions, however, remain to be addressed. First, under physiological conditions, CXCL8 exists as a mixture of dimer and monomer (52). It was previously shown that the monomeric and dimeric forms of CXCL8 differ in their ability to activate and regulate CXCR1 and CXCR2 (33). Thus, it is possible that the complexes monomer/receptor and dimer/receptor may couple to different GRK isoform to mediate and regulate cellular responses. Second, using receptor specific antibodies it was recently shown that phosphorylation of specific serine or threonine residues on the cytoplasmic tail of the β2-adrenergic receptor and CXCR4 by specific GRKs govern the ability of the receptors to complex with β–arrestins and modulate cellular activities (53). CXCR1 and CXCR2 possess several serine and threonine residues in their cytoplasmic tails, which are critical for receptor phosphorylation, desensitization, down-regulation, and post-endocytic activities (5). Thus, defining the specific role of these residues in receptor activation and regulation may provide new insights on the role of CXCL8 in inflammation, tumor progression and metastasis as well as new target for therapeutic interventions.

Acknowledgments

References

1. Baggiolini M. Reflections on chemokines. Immunol Rev. 2000; 177:5–7. [PubMed: 11138784]

2. Murphy PM, Baggiolini M, Charo IF, Hebert CA, Horuk R, Matsushima K, Miller LH, Oppenheim JJ, Power CA. International union of pharmacology. XXII. Nomenclature for chemokine receptors. Pharmacol Rev. 2000; 52:145–176. [PubMed: 10699158]

3. Baggiolini M, Dewald B, Moser B. Human chemokines: an update. Annu Rev Immunol. 1997; 15:675–705. [PubMed: 9143704]

4. Richardson RM, Pridgen BC, Haribabu B, Ali H, Snyderman R. Differential cross-regulation of the human chemokine receptors CXCR1 and CXCR2. Evidence for time-dependent signal generation. J Biol Chem. 1998; 273:23830–23836. [PubMed: 9726994]

5. Richardson RM, Marjoram RJ, Barak LS, Snyderman R. Role of the cytoplasmic tails of CXCR1 and CXCR2 in mediating leukocyte migration, activation, and regulation. J Immunol. 2003; 170:2904–2911. [PubMed: 12626541]

6. Yang W, Wang D, Richmond A. Role of clathrin-mediated endocytosis in CXCR2 sequestration, resensitization, and signal transduction. J Biol Chem. 1999; 274:11328–11333. [PubMed: 10196223]

7. Neel NF, Schutyser E, Sai J, Fan GH, Richmond A. Chemokine receptor internalization and intracellular trafficking. Cytokine Growth Factor Rev. 2005; 16:637–658. [PubMed: 15998596]

8. Vroon A, Heijnen CJ, Kavelaars A. GRKs and arrestins: regulators of migration and inflammation. J Leukoc Biol. 2006; 80:1214–1221. [PubMed: 16943386]

9. Reiter E, Lefkowitz RJ. GRKs and beta-arrestins: roles in receptor silencing, trafficking and signaling. Trends Endocrinol Metab. 2006; 17:159–165. [PubMed: 16595179]

10. Pitcher JA, Freedman NJ, Lefkowitz RJ. G protein-coupled receptor kinases. Annu Rev Biochem. 1998; 67:653–692. [PubMed: 9759500]

11. Premont RT, Gainetdinov RR. Physiological roles of G protein-coupled receptor kinases and arrestins. Annu Rev Physiol. 2007; 69:511–534. [PubMed: 17305472]

12. Cho D, Zheng M, Min C, Ma L, Kurose H, Park JH, Kim KM. Agonist-induced endocytosis and receptor phosphorylation mediate resensitization of dopamine D(2) receptors. Mol Endocrinol. 2010; 24:574–586. [PubMed: 20160122]

13. Sallese M, Salvatore L, D'Urbano E, Sala G, Storto M, Launey T, Nicoletti F, Knopfel T, De Blasi A. The G-protein-coupled receptor kinase GRK4 mediates homologous desensitization of metabotropic glutamate receptor 1. Faseb J. 2000; 14:2569–2580. [PubMed: 11099476]

14. Luo J, Busillo JM, Benovic JL. M3 muscarinic acetylcholine receptor-mediated signaling is regulated by distinct mechanisms. Mol Pharmacol. 2008; 74:338–347. [PubMed: 18388243]

15. de Jager SC, Bermudez B, Bot I, Koenen RR, Bot M, Kavelaars A, de Waard V, Heijnen CJ, Muriana FJ, Weber C, van Berkel TJ, Kuiper J, Lee SJ, Abia R, Biessen EA. Growth differentiation factor 15 deficiency protects against atherosclerosis by attenuating CCR2-mediated macrophage chemotaxis. J Exp Med. 2011; 208:217–225. [PubMed: 21242297]

16. Vroon A, Heijnen CJ, Lombardi MS, Cobelens PM, Mayor F Jr, Caron MG, Kavelaars A. Reduced GRK2 level in T cells potentiates chemotaxis and signaling in response to CCL4. J Leukoc Biol. 2004; 75:901–909. [PubMed: 14761932]

17. Kleibeuker W, Jurado-Pueyo M, Murga C, Eijkelkamp N, Mayor F Jr, Heijnen CJ, Kavelaars A. Physiological changes in GRK2 regulate CCL2-induced signaling to ERK1/2 and Akt but not to MEK1/2 and calcium. J Neurochem. 2008; 104:979–992. [PubMed: 17971124]

18. Zidar DA, Violin JD, Whalen EJ, Lefkowitz RJ. Selective engagement of G protein coupled receptor kinases (GRKs) encodes distinct functions of biased ligands. Proc Natl Acad Sci U S A. 2009; 106:9649–9654. [PubMed: 19497875]

19. Vroon A, Heijnen CJ, Raatgever R, Touw IP, Ploemacher RE, Premont RT, Kavelaars A. GRK6 deficiency is associated with enhanced CXCR4-mediated neutrophil chemotaxis in vitro and impaired responsiveness to G-CSF in vivo. J Leukoc Biol. 2004; 75:698–704. [PubMed: 14704365]

20. Busillo JM, Armando S, Sengupta R, Meucci O, Bouvier M, Benovic JL. Site-specific phosphorylation of CXCR4 is dynamically regulated by multiple kinases and results in differential modulation of CXCR4 signaling. J Biol Chem. 2010; 285:7805–7817. [PubMed: 20048153]

21. Prado GN, Suzuki H, Wilkinson N, Cousins B, Navarro J. Role of the C terminus of the interleukin 8 receptor in signal transduction and internalization. J Biol Chem. 1996; 271:19186–19190. [PubMed: 8702597]

22. Ben-Baruch A, Bengali KM, Biragyn A, Johnston JJ, Wang JM, Kim J, Chuntharapai A, Michiel DF, Oppenheim JJ, Kelvin DJ. Interleukin-8 receptor beta. The role of the carboxyl terminus in signal transduction. J Biol Chem. 1995; 270:9121–9128. [PubMed: 7721826]

23. Matityahu E, Feniger-Barish R, Meshel T, Zaslaver A, Ben-Baruch A. Intracellular trafficking of human CXCR1 and CXCR2: regulation by receptor domains and actin-related kinases. Eur J Immunol. 2002; 32:3525–3535. [PubMed: 12442335]

24. Ali H, Richardson RM, Tomhave ED, Didsbury JR, Snyderman R. Differences in phosphorylation of formylpeptide and C5a chemoattractant receptors correlate with differences in desensitization. J Biol Chem. 1993; 268:24247–24254. [PubMed: 8226971]

25. Nasser MW, Raghuwanshi SK, Malloy KM, Gangavarapu P, Shim JY, Rajarathnam K, Richardson RM. CXCR1 and CXCR2 activation and regulation. Role of aspartate 199 of the second extracellular loop of CXCR2 in CXCL8-mediated rapid receptor internalization. J Biol Chem. 2007; 282:6906–6915. [PubMed: 17204468]

26. Richardson RM, Pridgen BC, Haribabu B, Snyderman R. Regulation of the human chemokine receptor CCR1. Cross-regulation by CXCR1 and CXCR2. J Biol Chem. 2000; 275:9201–9208. [PubMed: 10734056]

27. Ali H, Tomhave ED, Richardson RM, Haribabu B, Snyderman R. Thrombin primes responsiveness of selective chemoattractant receptors at a site distal to G protein activation. J Biol Chem. 1996; 271:3200–3206. [PubMed: 8621721]

28. Nasser MW, Marjoram RJ, Brown SL, Richardson RM. Cross-desensitization among CXCR1, CXCR2, and CCR5: role of protein kinase C-epsilon. J Immunol. 2005; 174:6927–6933. [PubMed: 15905535]

29. Brown SL, Jala VR, Raghuwanshi SK, Nasser MW, Haribabu B, Richardson RM. Activation and regulation of platelet-activating factor receptor: role of G(i) and G(q) in receptor-mediated chemotactic, cytotoxic, and cross-regulatory signals. J Immunol. 2006; 177:3242–3249. [PubMed: 16920964]

30. Fong AM, Premont RT, Richardson RM, Yu YR, Lefkowitz RJ, Patel DD. Defective lymphocyte chemotaxis in beta-arrestin2- and GRK6-deficient mice. Proc Natl Acad Sci U S A. 2002; 99:7478–7483. [PubMed: 12032308]

31. Raghuwanshi SK, Nasser MW, Chen X, Strieter RM, Richardson RM. Depletion of beta-arrestin-2 promotes tumor growth and angiogenesis in a murine model of lung cancer. J Immunol. 2008; 180:5699–5706. [PubMed: 18390755]

32. Su Y, Raghuwanshi SK, Yu Y, Nanney LB, Richardson RM, Richmond A. Altered CXCR2 signaling in beta-arrestin-2-deficient mouse models. J Immunol. 2005; 175:5396–5402. [PubMed: 16210646]

33. Nasser MW, Raghuwanshi SK, Grant DJ, Jala VR, Rajarathnam K, Richardson RM. Differential activation and regulation of CXCR1 and CXCR2 by CXCL8 monomer and dimer. J Immunol. 2009; 183:3425–3432. [PubMed: 19667085]

34. Edwards JC, Sedgwick AD, Willoughby DA. The formation of a structure with the features of synovial lining by subcutaneous injection of air: an in vivo tissue culture system. J Pathol. 1981; 134:147–156. [PubMed: 7019400]

35. Sin YM, Sedgwick AD, Chea EP, Willoughby DA. Mast cells in newly formed lining tissue during acute inflammation: a six day air pouch model in the mouse. Ann Rheum Dis. 1986; 45:873–877. [PubMed: 3789822]

36. Clish CB, O'Brien JA, Gronert K, Stahl GL, Petasis NA, Serhan CN. Local and systemic delivery of a stable aspirin-triggered lipoxin prevents neutrophil recruitment in vivo. Proc Natl Acad Sci U S A. 1999; 96:8247–8252. [PubMed: 10393980]

37. Devalaraja RM, Nanney LB, Du J, Qian Q, Yu Y, Devalaraja MN, Richmond A. Delayed wound healing in CXCR2 knockout mice. J Invest Dermatol. 2000; 115:234–244. [PubMed: 10951241]

38. Milatovic S, Nanney LB, Yu Y, White JR, Richmond A. Impaired healing of nitrogen mustard wounds in CXCR2 null mice. Wound Repair Regen. 2003; 11:213–219. [PubMed: 12753603]

39. Nanney BL. Epidermal and dermal effects of epidermal growth factor during wound repair. J Invest Dermatol. 1990; 94:624–629. [PubMed: 2324518]

40. Thorey IS, Hinz B, Hoeflich A, Kaesler S, Bugnon P, Elmlinger M, Wanke R, Wolf E, Werner S. Transgenic mice reveal novel activities of growth hormone in wound repair, angiogenesis, and myofibroblast differentiation. J Biol Chem. 2004; 279:26674–26684. [PubMed: 15070902]

41. Damaj BB, McColl SR, Neote K, Hebert CA, Naccache PH. Diverging signal transduction pathways activated by interleukin 8 (IL-8) and related chemokines in human neutrophils. IL-8 and Gro-alpha differentially stimulate calcium influx through IL-8 receptors A and B. J Biol Chem. 1996; 271:20540–20544. [PubMed: 8702797]

42. Richardson RM, DuBose RA, Ali H, Tomhave ED, Haribabu B, Snyderman R. Regulation of human interleukin-8 receptor A: identification of a phosphorylation site involved in modulating receptor functions. Biochemistry. 1995; 34:14193–14201. [PubMed: 7578017]

43. Feniger-Barish R, Ran M, Zaslaver A, Ben-Baruch A. Differential modes of regulation of cxc chemokine-induced internalization and recycling of human CXCR1 and CXCR2. Cytokine. 1999; 11:996–1009. [PubMed: 10623425]

44. Barlic J, Andrews JD, Kelvin AA, Bosinger SE, DeVries ME, Xu L, Dobransky T, Feldman RD, Ferguson SS, Kelvin DJ. Regulation of tyrosine kinase activation and granule release through beta-arrestin by CXCRI. Nat Immunol. 2000; 1:227–233. [PubMed: 10973280]

45. Chuntharapai A, Kim KJ. Regulation of the expression of IL-8 receptor A/B by IL-8: possible functions of each receptor. J Immunol. 1995; 155:2587–2594. [PubMed: 7650389]

46. Guo Q, Subramanian H, Gupta K, Ali H. Regulation of C3a receptor signaling in human mast cells by G protein coupled receptor kinases. PLoS One. 2011; 6:e22559. [PubMed: 21799898]

47. Vibhuti A, Gupta K, Subramanian H, Guo Q, Ali H. Distinct and shared roles of beta-arrestin-1 and beta-arrestin-2 on the regulation of C3a receptor signaling in human mast cells. PLoS One. 2011; 6:e19585. [PubMed: 21589858]

48. Zhao M, Wimmer A, Trieu K, Discipio RG, Schraufstatter IU. Arrestin regulates MAPK activation and prevents NADPH oxidase-dependent death of cells expressing CXCR2. J Biol Chem. 2004; 279:49259–49267. [PubMed: 15364949]

49. Ren XR, Reiter E, Ahn S, Kim J, Chen W, Lefkowitz RJ. Different G protein-coupled receptor kinases govern G protein and beta-arrestin-mediated signaling of V2 vasopressin receptor. Proc Natl Acad Sci U S A. 2005; 102:1448–1453. [PubMed: 15671180]

50. Fan GH, Yang W, Wang XJ, Qian Q, Richmond A. Identification of a motif in the carboxyl terminus of CXCR2 that is involved in adaptin 2 binding and receptor internalization. Biochemistry. 2001; 40:791–800. [PubMed: 11170396]

51. Barker BL, Benovic JL. G protein-coupled receptor kinase 5 phosphorylation of hip regulates internalization of the chemokine receptor CXCR4. Biochemistry. 2011; 50:6933–6941. [PubMed: 21728385]

52. Burrows SD, Doyle ML, Murphy KP, Franklin SG, White JR, Brooks I, McNulty DE, Scott MO, Knutson JR, Porter D, et al. Determination of the monomer-dimer equilibrium of interleukin-8 reveals it is a monomer at physiological concentrations. Biochemistry. 1994; 33:12741–12745. [PubMed: 7947677]

53. Tran TM, Jorgensen R, Clark RB. Phosphorylation of the beta2-adrenergic receptor in plasma membranes by intrinsic GRK5. Biochemistry. 2007; 46:14438–14449. [PubMed: 18034461]

Abbreviations used in this paper

GRK	G protein coupled receptor kinase
GPCR	G protein-coupled receptor
βarr2	β-arrestin-2
CXCL8/IL-8	interleukin-8
CXCR2	IL-8 receptor B
ELR	Glu-Leu-Arg
KC or CXCL1	keratinocyte-derived chemokine
RBL	rat basophilic leukemia
VEGF	vascular endothelial growth factor
MMPs	matrix metalloproteinases
MPO	Myeloperoxidase

MAP kinase mitogen-activated protein kinase
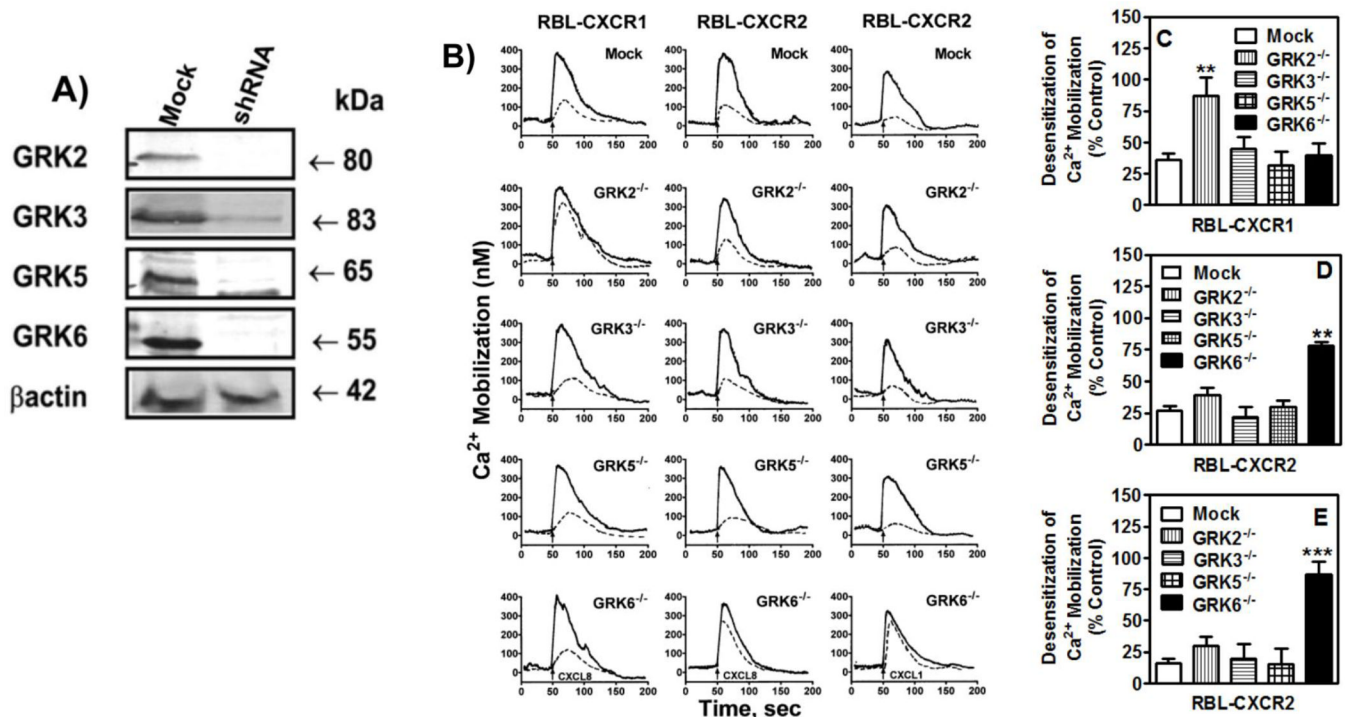
ERK Extracellular signal-regulated kinases

Figure 1. Transient inhibition of GRK2, GRK3, GRK5 and GRK6 expression in RBL-2H3 cells and their effects in CXCR1 and CXCR2 desensitization

A) RBL cells (5×10^5 cells/well) were transfected with 20 μg of control (mock) or siRNA specific for GRK2, GRK3, GRK5 or GRK6. Forty-eight h post transfection, cells were lysed and analyzed by immunoblotting. **B)** For receptor desensitization, GRK deficient and control (mock transfected) RBL cells (5×10^6 cells) expressing CXCR1 or CXCR2 were loaded with Indo-1 in the presence or absence of 10 nM CXCL8 (left and middle columns) or CXCL1 (right column) for 30 min and assayed for CXCL8 or CXCL1 (10 nM) induced intracellular Ca^{2+} mobilization. Traces shown are representative of 3–5 experiments. **C, D and E)** Desensitization were determined as percentage of control which is the peak of intracellular Ca^{2+} mobilization obtained in the absence of pretreatment. Data shown are average of at least 3 traces. Statistical difference is evaluated by Student's t test. ***P<0.01; *** P < 0.001.*
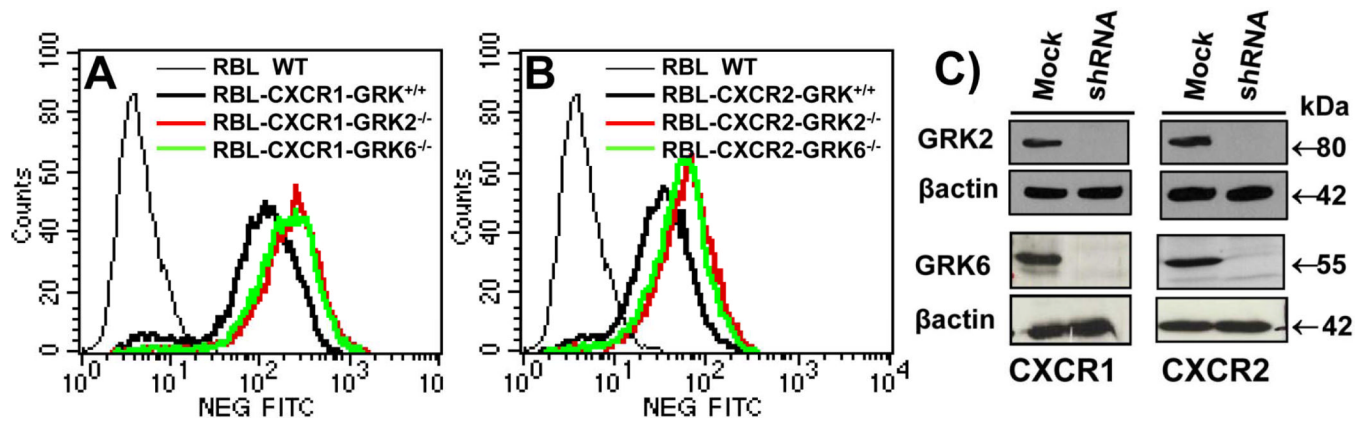
Figure 2. Stable knockdown of GRK2 and GRK6 expression in RBL-2H3 cells stably expressing CXCR1 and CXCR2

A & B) A representative histogram of FACS analysis showing surface expression of CXCR1 **(A)** and CXCR2 **(B)** in RBL-2H3 cells after staining with CXCR1 or CXCR2 specific antibodies. **B)** RBL-2H3 cells expressing CXCR1 (left panel) or CXCR2 (right panel) were transfected with scrambled shRNA control lentivirus (mock) or shRNA lentivirus specific for GRK2 or GRK6 knockdown. Puromycin resistant cells were selected and single clones were generated and analyzed by immunoblotting.
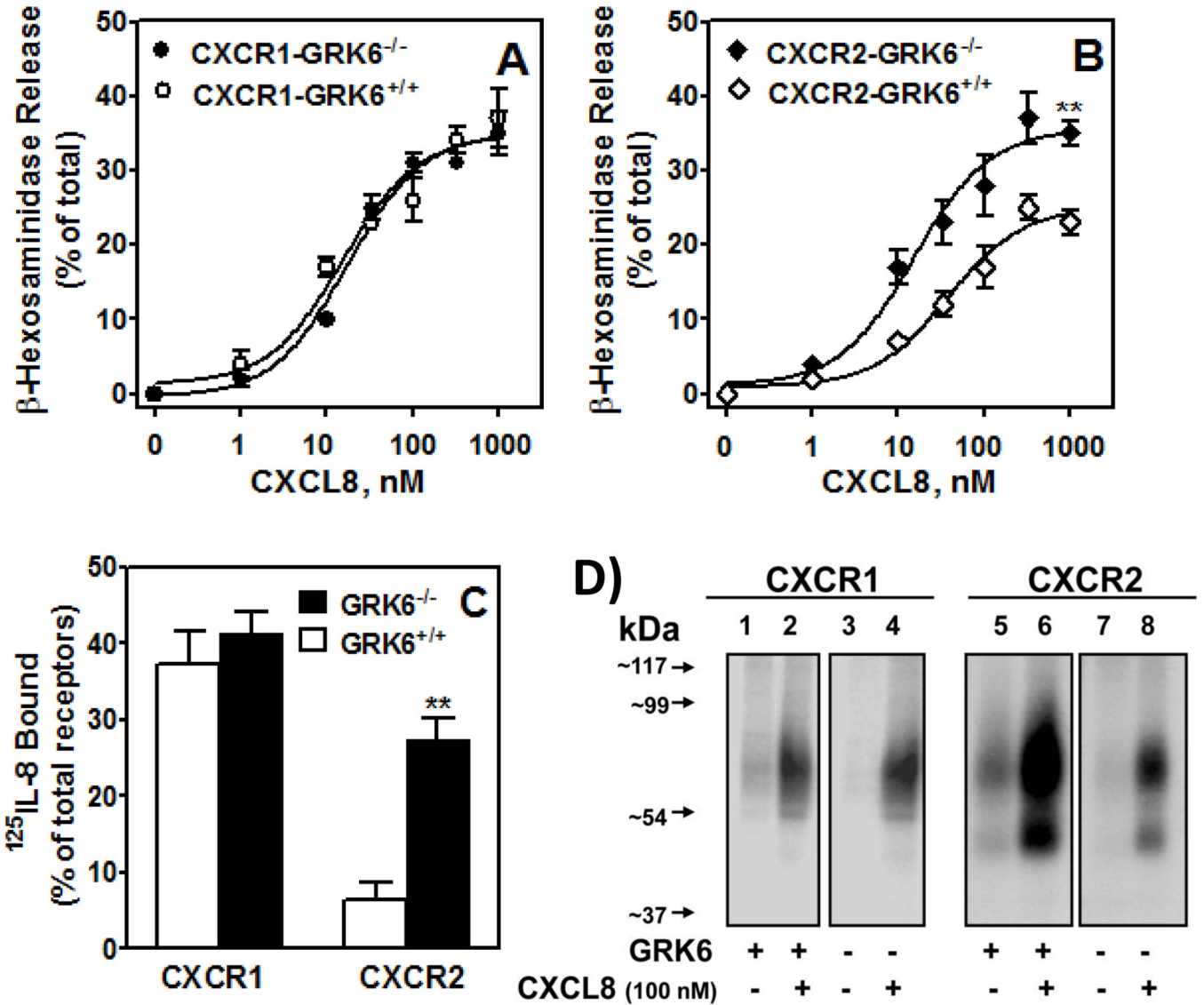
Figure 3. GRK6 inhibition enhances CXCR2-mediated exocytosis and decreases receptor phosphorylation and internalization

A & B) For β-hexosaminidase release, cells (50,000/well) were cultured overnight, washed with HEPES-buffered saline and stimulated with different concentrations of CXCL8 for 10 min. Supernatant (15 μl) was removed, and β-hexosaminidase release was measured. Data are represented as percentage of total β-hexosaminidase release from cell lysates. The experiments were repeated four times with similar results. *$**P<0.01$*. **C**) For receptor internalization, cells (0.5×10^6/well) were treated with CXCL8 (100 nM) or vehicle control for 60 min and assayed for ^{125}I-CXCL8 binding. Data are represented as percentage of total ^{125}I-CXCL8 bound to control (untreated) cells. *$**P<0.01$*. **D**) For receptor phosphorylation, ^{32}P-labeled GRK6$^{+/+}$ (lanes 1 & 2) and GRK6$^{-/-}$ (lanes 3 & 4) RBL cells (5×10^6 cells/60 mm plate) expressing CXCR1 (left panels) or CXCR2 (right panels) were incubated for 5 min with (lanes 2 & 4) or without (lanes 1 & 3) 100 nM CXCL8. Cells were lysed, immunoprecipitated with CXCR1 and CXCR2 antibodies, analyzed by SDS-PAGE, and autoradiographed. The results shown are from a representative experiment that was repeated twice.
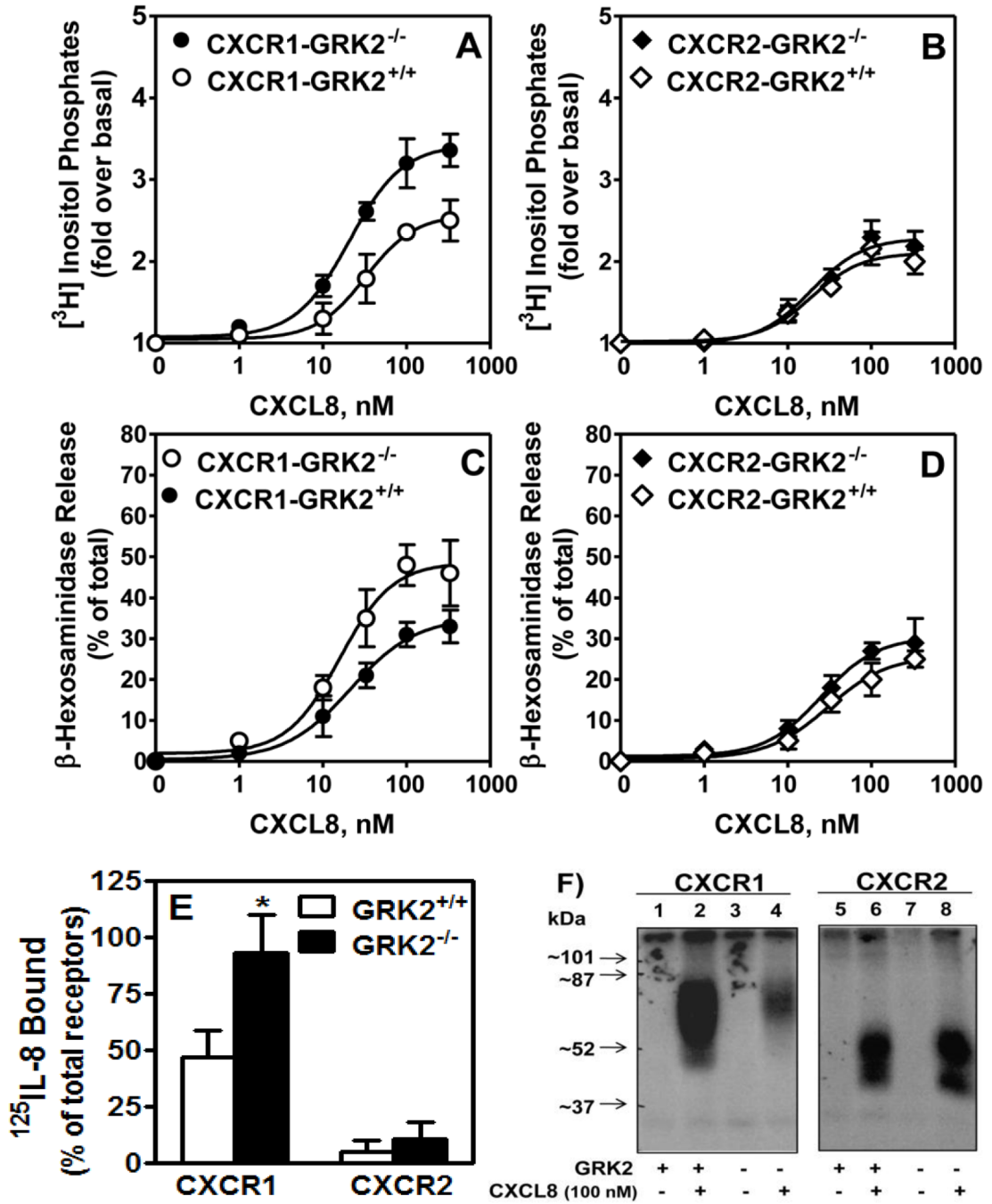
Figure 4. GRK2 knockdown increases CXCR1-mediated exocytosis but decreases receptor phosphorylation and internalization

For the generation of inositol phosphates (**A and B**), cells (50,000/well) were cultured overnight in the presence of [^{3}H]inositol (1 μC/ml), washed with HEPES-buffered saline, pre-incubated for 10 min at 37°C with HEPES-buffered saline containing 10 mM LiCl in a total volume of 200μl and stimulated with different concentrations of CXCL8 for 10 min. The supernatant was used to determine the release of inositol phosphates. Data are represented as the fold stimulation over basal. β-hexosaminidase release (**C & D**) was measured as described in the legend of Fig. 3A and B. Data are represented as fold over basal PI (**A & B**), or percentage of total β-hexosaminidase release from cell lysates (**C &**

D). Data shown are average of three experiments performed in triplicate. Receptor internalization (**E**) and phosphorylation (**F**) were measured as described in the legend of Figure 3. The results are average (**E**) or a representative (**F**) of three experiments. * $p < 0.05$, Student's t test.
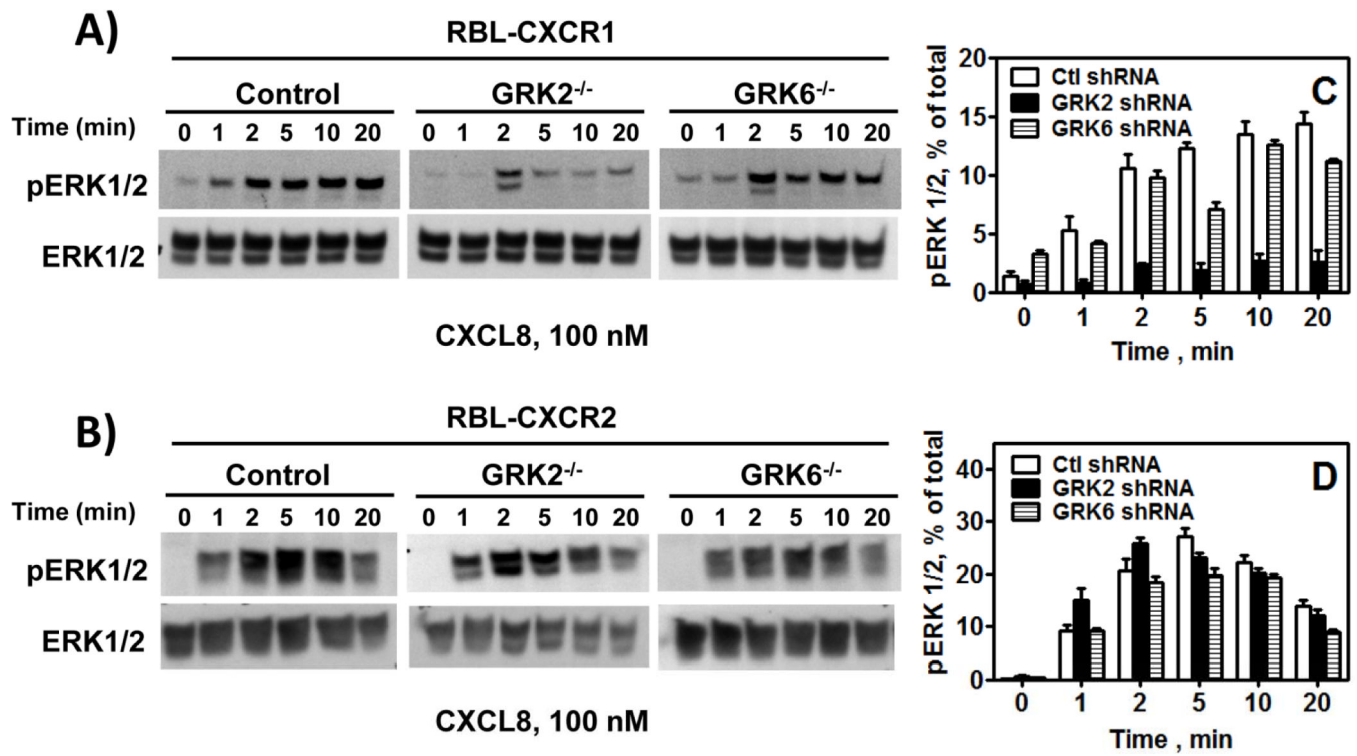
Figure 5.
Effect of GRK2 and GRK6 knockdown in CXCR1 and CXCR2-induced ERK1/2 phosphorylation: RBL-2H3 cells were stimulated with CXCL8 (100 nM) for 0–20 min. ERK1/2 phosphorylation and total ERK were determined by Western blotting using anti-phospho-ERK1/2 (pERK1/2) and anti-total ERK1/2 (ERK1/2) antibodies, respectively. Results shown are % of total ERK and are average of 3 experiments.
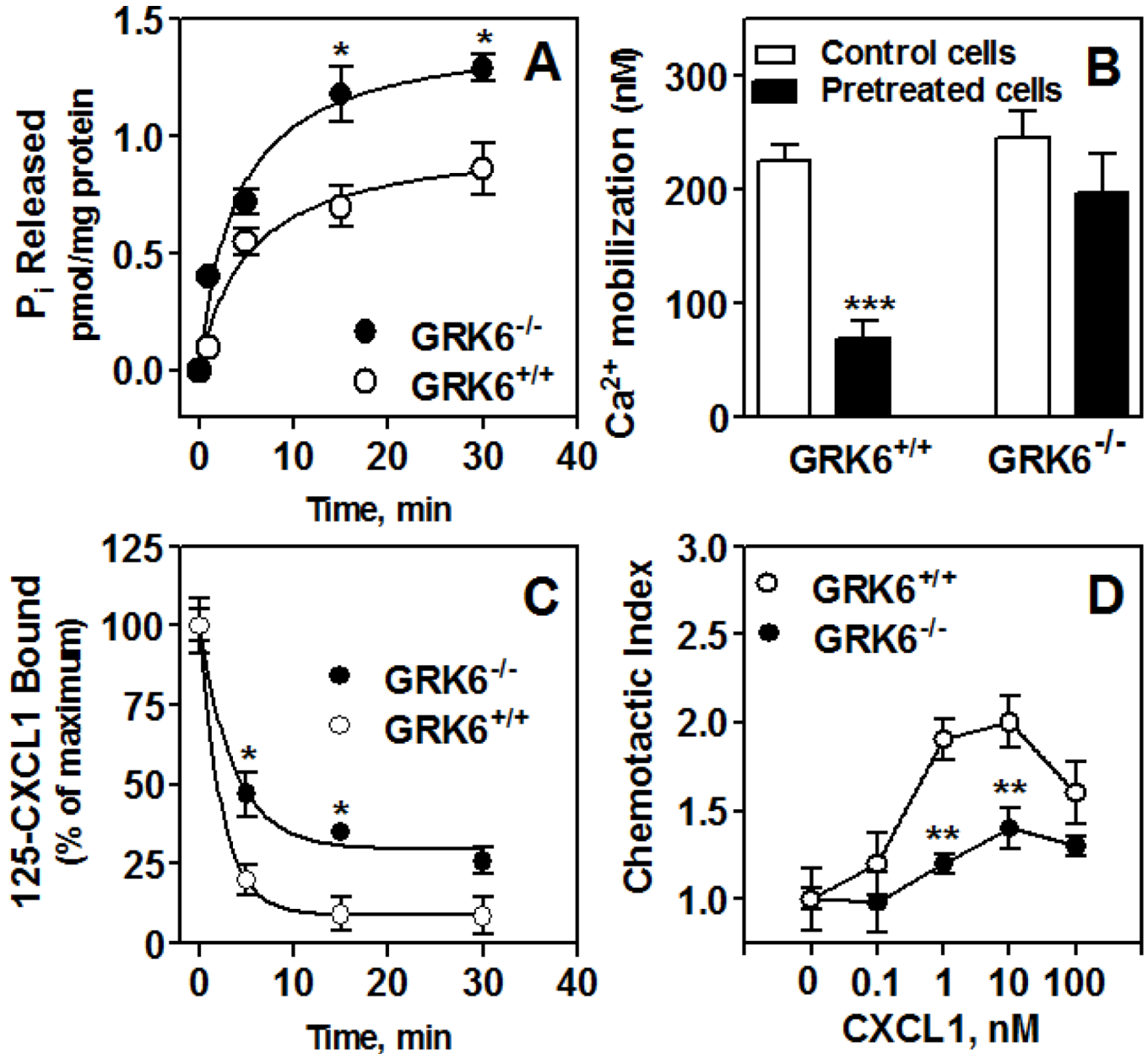
Figure 6.
CXCL1-induced GTPase activity (A), intracellular Ca^{2+} mobilization (B), chemotaxis (D) and receptor internalization (C) in neutrophils from mice deficient in GRK6 ($GRK6^{-/-}$) relative to wild type ($GRK6^{+/+}$). Zymosan-elicited peritoneal neutrophils were collected from mice deficient in GRK6 ($GRK6^{-/-}$) and control littermates ($GRK6^{+/+}$). **A)** Membranes were prepared from zymosan-elicited peritoneal neutrophils and assayed for time-dependent CXCL1-stimulated Pi released. Results shown are representative of one of two experiments performed in triplicate. *P<0.05; **P<0.01,* Student's t test. **B)** Cells (3×10^6 cells) were Indo-1–loaded pretreated with or without CXCL1 (100 nM) and stimulated with 10 nM CXCL1. The data shown are representative of at least 3 traces. **C)** Cells (0.5×10^6 cells) were treated with CXCL1 (100 nM) for different period of time and assayed for ^{125}I-CXCL1 binding. Data are represented as percentage of total ^{125}I-CXCL8 bound to control (untreated) cells. *P<0.01,* Student's t test. **D)** Cells were incubated with calcein AM

ionophore for 30 min and resuspended (1.0×10^5/20ml) in RPMI without phenol red. Different concentrations of CXCL8 were loaded in a neuroprobe 96-well plate. The cells were added to the top of the filter and incubated for 2 h at 37 °C. After incubation, the top of the filter was washed five times with medium and fluorescence intensity of the bottom well-plate was measured in a Perkin Elmer fluorescence microplate reader. The experiment was repeated 3 times in triplicate. ***P<0.01; *** P < 0.001,* Student's t test.
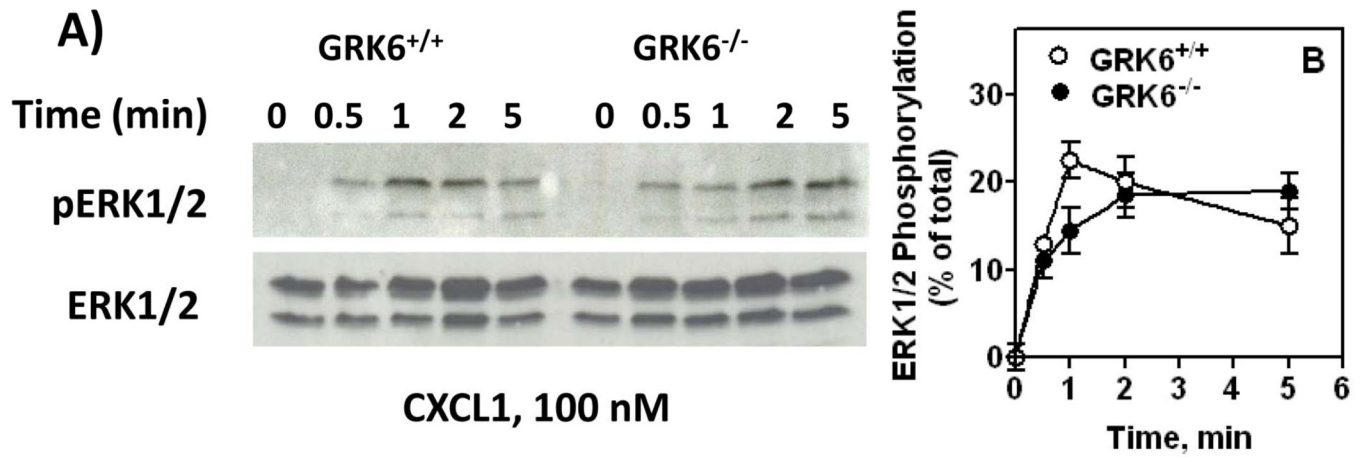
Figure 7.
CXCL1-induced ERK activity. Zymosan-elicited peritoneal neutrophils from GRK6$^{-/-}$ and GRK6$^{+/+}$ mice were treated with CXCL1 for different periods of time. Cell lysates were assayed for ERK phosphorylation using phospho-ERK antibody. Results shown are % of total ERK and are average of 3 experiments.
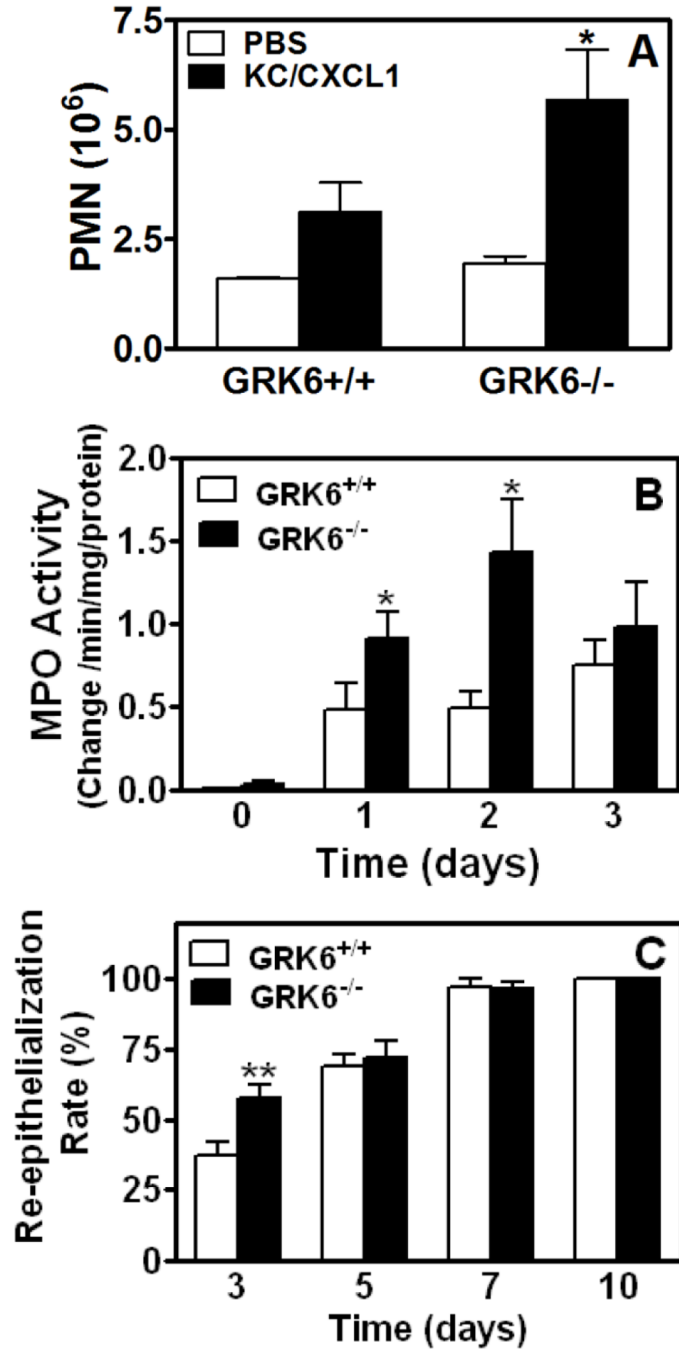
Figure 8.
Effect of GRK6 knockdown in leukocyte migration, myeloperoxidase (MPO) activity and wound re-epithelialization. **A**) Six-day air pouches were raised in the dorsum of 6–8 week old GRK6$^{-/-}$ mice and their littermates (GRK6$^{+/+}$). Mice were injected with 0.5 ml PBS or PBS containing murine CXCL1 (100 pmol). Exudates were collected after 4 h and the total number of leukocytes (~90% neutrophils) was enumerated. *$P<0.05$, Student's t test. **B**) Wound extracts from GRK6$^{-/-}$ and wild type GRK6$^{+/+}$ mice were harvested and MPO activity within each wound bed was determined spectrophotometrically. The mean ± SEM value of four wounds for each time point of each mouse genotype is shown. Statistical

difference is evaluated by Student's t test. *P<0.05.* **C)** Percentage of epidermal re-surfacing for wounds from wild type GRK6$^{+/+}$ and GRK6$^{-/-}$ animals were measured at days 3, 5, 7 and 10 as described in Materials and Methods. The value of each time point was obtained from 8 wounds and is expressed as mean ± SEM. ** p<0.01 by Student's t-test.